RSC Advances

PAPER

View Article Online
View Journal | View Issue

Cite this: *RSC Adv.*, 2020, **10**, 44728

Sustainable separation of bio-based cadaverine based on carbon dioxide capture by forming carbamate†

Hui Li,[a] Xu Xu,[a] Weimin Tan,[b] Xuedong Lu,[a] Feng He,[c] Sheng Xu,[a] Weilong Tian,[c] Kequan Chen,[a]* Ganlu Li,[a]* Pingkai Ouyang,[a] Yaozong Liu[d] and Ruiyuan Liang[d]

Received 8th October 2020
Accepted 8th November 2020

DOI: 10.1039/d0ra08564b

rsc.li/rsc-advances

Bio-based cadaverine, manufactured by the decarboxylation of L-lysine, is an important raw material. However, the extractive-distillation separation and purification of cadaverine from bioconversion fluids require high energy consumption and leads to the loss of self-released carbon dioxide during the decarboxylation of L-lysine. This study focuses on the green and sustainable separation of bio-based cadaverine based on the capture of self-released carbon dioxide by cadaverine forming carbamate. Results showed that granular-activated carbon JK1 shows the best decolorization efficiency and achieves a higher cadaverine yield. After three times of solventing-out crystallization, refined cadaverine carbamate with 99.1% purity and total 57.48% yield was obtained. It was also found that the refined cadaverine carbamate consists of mixed crystals having numerous structural forms that can easily dissociate carbon dioxide. Furthermore, the amine carbamate strategy may be of great value for the development of a green and sustainable separation mode of bio-based amines and carbon dioxide capture.

Cadaverine (1,5-diaminopentane) is a natural five-carbon diamine prepared *via* the decarboxylation of L-lysine catalyzed by L-lysine decarboxylase.[1,2] A bio-based cadaverine monomer is mainly manufactured *via* the whole-cell bioconversion or direct microbial fermentation on a laboratory scale or scale-up.[3–5] Several engineered strains are constructed to catalyze the decarboxylation of L-lysine to manufacture cadaverine *via* whole-cell bioconversion.[6–8] However, the process of manufacturing bio-based cadaverine using L-lysine as a substrate releases equal moles of greenhouse gas carbon dioxide.[9] Excessive emission of carbon dioxide in chemical processes is leading to an ever increasing imbalance in the atmospheric circulation of carbon dioxide.[10,11] Therefore, the utilization of carbon dioxide as the one-carbon building block for the synthesis of high-value chemicals offers the opportunity to bring sustainable economic value and environmental benefits.

Bio-based cadaverine, an important chemical raw material, can be used to replace synthesized petrochemical 1,6-hexanediamine, in the polymer chemistry for the preparation of polyurethanes, adhesives, and coatings.[12–16] Organic solvent-based liquid–liquid extraction, such as *n*-butanol, isoamyl alcohol, hexane, methyl ethyl ketone, and methyl isobutyl ketone, is often used to separate cadaverine from the bioconversion fluid or fermentation media and then to further purify it by distillation.[17–19] However, the extractive-distillation separation and purification of cadaverine from the bioconversion fluid or fermentation media requires high energy consumption and leads to the loss of self-released carbon dioxide in the decarcboxylation process of L-lysine.[20,21] The amine within a base organic solvent system can react with carbon dioxide to form carbamate. Numerous monoamines and diamines, such as piperazine, ammonia, diglycolamine, and amino acids form carbamates by the capture of carbon dioxide.[22–25] However, there are few reports on the sustainable separation and purification of bio-based cadaverine from bioconversion fluid or fermentation media based on the carbon dioxide capture *via* the formation of carbamate. Therefore, the preparation of cadaverine carbamate in the extraction solution containing deprotonated cadaverine can not only utilize the self-released carbon dioxide in the decarboxylation process of L-lysine but also avoid the high energy consumption of the distillation process, which has the potential for green and sustainable economic benefits.

To summarize, in this study, a green and sustainable preparation technology of bio-based cadaverine carbamate from a bioconversion fluid was developed, as shown in Scheme 1. First, the cadaverine bioconversion fluid with a concentration of

[a]*College of Biotechnology and Pharmaceutical Engineering, Nanjing Tech University, Nanjing, 211816, China. E-mail: kqchen@njtech.edu.cn; tkscb@163.com*

[b]*National Engineering Research Center for Coatings, CNOOC Changzhou Paint and Coatings Industry Research Institute Co., Ltd., Changzhou, 213016, China*

[c]*Jiangsu Jicui Industrial Biotechnology Research Institute Co., Ltd, Nanjing, 210000, China*

[d]*Gansu Yinguang Juyin Chemical Co., Ltd, Baiyin, Gansu, 730900, China*

† Electronic supplementary information (ESI) available. See DOI: 10.1039/d0ra08564b

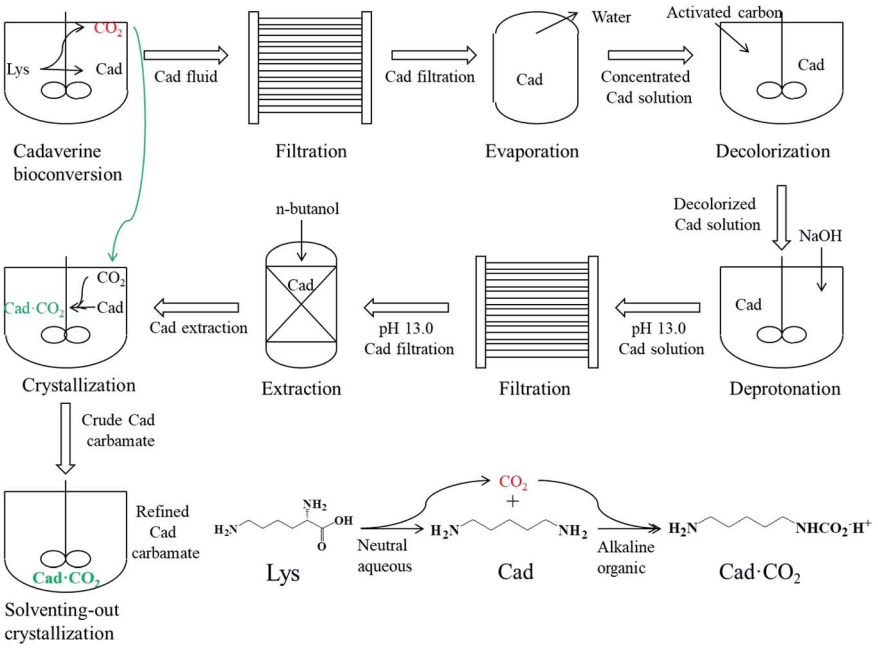

Scheme 1 Preparation process of cadaverine carbamate.

150 g L^{-1} was filtered by a microfiltration system to remove the cells and protein impurities, followed by the collection of the cadaverine microfiltration solution. Then, the concentrated cadaverine solution with a concentration of 450 g L^{-1} was obtained *via* vacuum evaporation to remove the extra water from the cadaverine microfiltration solution. After that, activated carbon was used to remove the pigment from the concentrated cadaverine solution. Further, the deprotonation reaction was carried out by adding NaOH into the decolorized concentrated cadaverine solution, and the precipitates were removed *via* filtration using a filter paper. Later, cadaverine was extracted using *n*-butanol in a volume ratio of 1 : 1 for three times from the deprotonated concentrated cadaverine solution, and the deprotonated cadaverine extraction solution was collected. Finally, carbon dioxide was injected into the deprotonated cadaverine extraction solution to form the crude carbamate, and then the refined cadaverine carbamate was obtained by solventing-out crystallization with ethanol for three times. This study provides a new idea for the separation of other bio-based amines, and carbamate can be used as intermediates for numerous high-value chemicals. Hopefully, this green technology can promote the development of biochemical industry.

Activated carbon with high porosity, surface area, and thermal stability, as a widely used industrial adsorbent, is often used in the decolorization process of biochemical raw materials.[26,27] Activated carbon, also known as the carbon molecular sieve, is a strong carbon adsorbent, divided into granular activated carbon and powder activated carbon.[28] Here, granular-activated carbon (JK1 and JK2) and powder-activated carbon (SF1 and SF2) are studied for the decolorization efficiency and cadaverine yield from the concentrated cadaverine solution, and the results are shown in Fig. 1. It is noted that granular activated carbon JK1 shows the best decolorization efficiency (88.28%) and maintains a higher cadaverine yield (98.30%), followed by JK2. Results also show that the granular activated carbon has the higher adsorption efficiency for pigment than the powder activated carbon. Compared with the powder activated carbon, the granular activated carbon has more regular structure and higher specific surface area, which is more conducive for the adsorption of pigment from raw materials.

In the decolorization process, appropriate dosage of the decolorant can not only obtain high decolorization efficiency but also control the cost.[29,30] The effects of 0.5, 1.0, 1.5, 2.0, and 2.5% (wt) of the granular activated carbon JK1 on the decolorization efficiency and cadaverine yield from the concentrated cadaverine solution are investigated, as shown in Fig. 2a. There is a positive correlation between the decolorization efficiency and the dosage of activated carbon added within the range of 0.5–2.5%, and a negative correlation between the cadaverine

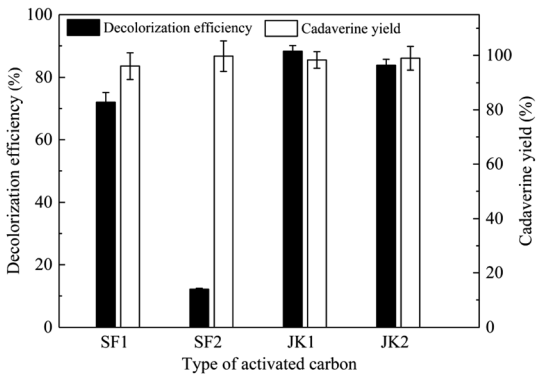

Fig. 1 Effects of activated carbon types on the decolorization efficiency and cadaverine yield in the concentrated cadaverine solution.

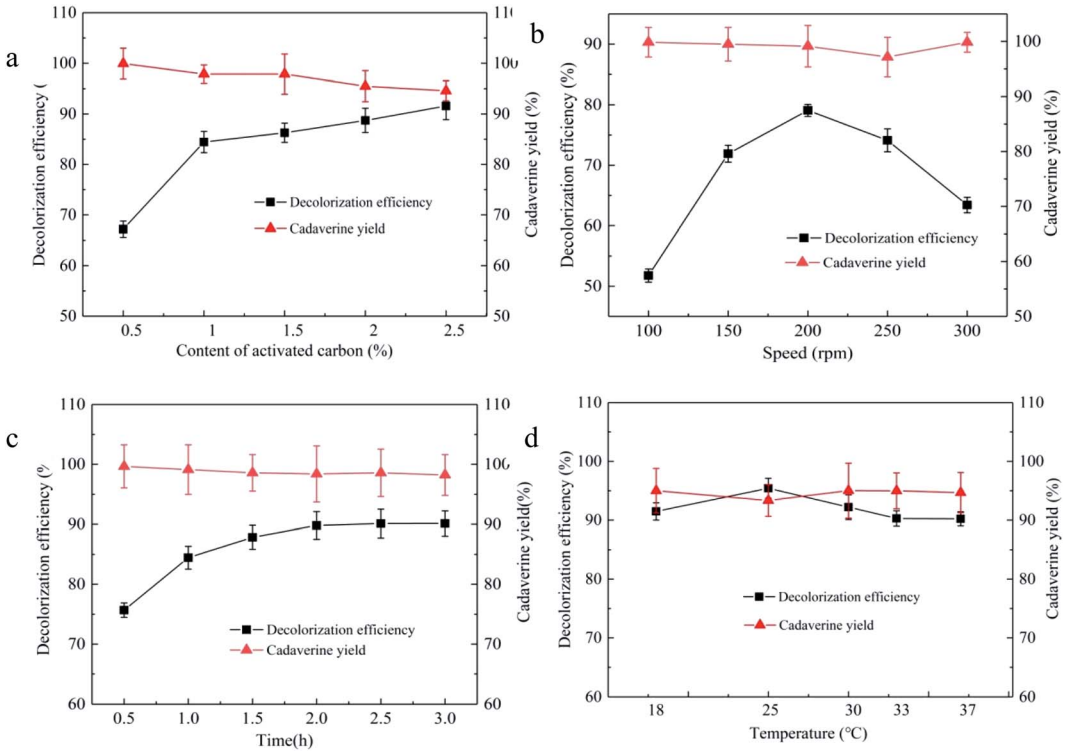

Fig. 2 Effects of the content of activated carbon (a), decolorization speed (b), decolorization time (c), and decolorization temperature (d) on decolorization efficiency and cadaverine yield in the concentrated cadaverine solution.

yield and the dosage of activated carbon added. According to the decolorization efficiency and cadaverine yield, the optimum addition level of the granular activated carbon JK1 was 1%, and the decolorization efficiency and cadaverine yield were 84.44% and 97.86%, respectively. The adsorption capacity of the adsorbent to the substrate and the pigment increases with the increase in the addition level of the adsorbent.[31]

The decolorization process needs proper mixing to promote the solid–liquid two-phase contact for carrying out the adsorption reaction by improving mass transfer. Stirring is an important way to mix well; however, the inappropriate stirring speed would have a great negative impact on the adsorption efficiency. Therefore, stirring speeds of 100, 150, 200, 250, and 300 rpm were selected to optimize the decolorization efficiency and cadaverine yield from the concentrated cadaverine solution. As shown in Fig. 2b, the stirring speed of 200 rpm in the decolorization process of the granular activated carbon JK1 shows the best decolorization efficiency of 79.09% and cadaverine yield of 99.1%. In addition, it was shown that increasing or decreasing stirring speed both decrease the decolorization efficiency. Low stirring speed would increase the adsorption time that in turn increases the cost, while high stirring speed results in poor decolorization effect due to the high shear stress.[32]

In order to avoid the decrease in decolorization efficiency caused by the long time decolorization process, decolorization times of 0.5, 1.0, 1.5, 2.0, 2.5, and 3.0 h for the granular activated carbon JK1 were selected to optimize the decolorization efficiency and cadaverine yield from the concentrated cadaverine solution, as shown in Fig. 2c. The decolorization efficiency is positively correlated with the decolorization time within the range of 0.5–2.0 h, and remains unchanged in the range of 2.0–3.0 h; however, the cadaverine yield is negatively correlated with the decolorization time. The decolorization time of 2.0 h shows the best decolorization efficiency of 89.80% with the cadaverine yield of 98.40%. The decolorization process, as a reversible process, would reach the adsorption equilibrium at the right time. Moreover, as time goes on, small pigment impurities are no longer adsorbed.[33,34]

The adsorption process of activated carbon is affected by temperature.[35] Therefore, decolorization temperatures of 18, 25, 30, 33, and 37 °C of the granular activated carbon JK1 were selected to optimize the decolorization efficiency and cadaverine yield, as shown in Fig. 2d. It is found that the decolorization efficiency of 95.42% is the highest at 25 °C with a cadaverine yield of 93.34%. With the increase in the decolorization temperature, decolorization efficiencies decrease continuously, which show that the pigment adsorption process of the granular activated carbon JK1 may be spontaneous exothermic process. At a low temperature, larger micropores and mesopores of the activated carbon may be favorable for the adsorption of the substrate and the pigment. However, at ambient temperature, smaller micropores of the activated carbon are favorable for the adsorption of the substrate and pigment.[35] The adsorption effect of the mesopores and micropores of activated carbon can be brought into full play at an appropriate temperature.

Amine absorption is currently one of the most promising technologies for the capture of carbon dioxide. The form of carbamate due to the carbon dioxide absorption by the usage of amine is preferred to increase the carbon dioxide loading capacity. The formation of carbamate requires the amino group of cadaverine to be in the molecular state; hence, the deprotonation reaction of the ionic state of cadaverine is necessary.[36] Simultaneously, the organic solvent can only extract the molecular state of cadaverine. Liquid–liquid extraction is often used to extract bio-based organic amine or acid from the bioconversion liquid or fermentation media.[37–39] According to the published reports, *n*-butanol is used as an extraction solvent for the extraction of cadaverine from the deprotonated concentrated cadaverine solution.

Carbon dioxide from the decarboxylation of L-lysine is introduced into the extraction solution of *n*-butanol containing deprotonated cadaverine. Carbon dioxide reacts directly with the amino group of cadaverine to form carbamate in the base *n*-butanol extraction solution. Cadaverine concentrations of 60.4, 134.2, and 272.0 g L^{-1} in the *n*-butanol extraction solution were chosen to investigate the formation of carbamate. The yield of crude cadaverine carbamate in the deprotonated cadaverine concentration of 60.4, 134.2, and 272.0 g L^{-1} in the *n*-butanol extraction solution are 94.1, 94.5 and 95.3%, respectively, as shown in Fig. 3, and the purity of crude cadaverine carbamate were 92.5, 91.7 and 90.7%, respectively. The cadaverine carbamate is precipitated as solid, indicating that it is insoluble in organic solvents. Purities of the crude cadaverine carbamate decrease with the increase in the concentration of deprotonated cadaverine in the *n*-butanol extraction solution. It is possible that the high concentration of cadaverine carbamate could cause water crystallization and entrainment of impurities during the preparation process of cadaverine carbamate by carbon dioxide capture.

It is found that the purity of crude cadaverine carbamate is low, so it is necessary to refine the crude cadaverine carbamate. Solventing-out crystallization is a common separation and purification method, and is widely used in the chemical, pharmaceutical, and food fields.[40] Here, solventing-out crystallization was used to refine the crude cadaverine carbamate. Solventing-out crystallization has the advantages of low cost, environment-friendliness and easy recovery of the solvent-out solvent.[41] The solventing-out crystallization process is divided into dissolution process and crystallization process. The dissolution process is to dissolve the solute in a solvent (called the main solvent) to form a saturated solution; the crystallization process is driven by the addition of a second solvent (anti-solvent or solvent-out solvent) that can completely dissolve the main solvent but cannot dissolve the solute, so that the solute is crystallized and precipitated.

Crude cadaverine carbamate was refined once, and the yield and purity of the cadaverine carbamate were 83.5% and 96.3%, respectively. Due to the partial dissolution of cadaverine carbamate in the main solvent (water), the yield of cadaverine carbamate is only 83.5%. There are hydrophilic phases and hydrophobic phases in the solventing-out crystallization system, so the impurities in the crude cadaverine carbamate are dissolved into the hydrophilic phase due to the principle of "similar solubility", which results in the separation of impurities and cadaverine carbamate. The cadaverine carbamate was dissolved and crystallized for three times, and the results are shown in Fig. 4. After three times of refinements, the cadaverine carbamate of 99.1% purity was obtained with a total yield of 57.48%. The contents of the C, N, O, and H elements in the refined cadaverine carbamate were determined as 49.22%, 19.30%, 22.49%, and 8.68%, respectively. Moreover, based on the elemental content, we calculated that the molar ratio of C : N : O : H in the refined cadaverine carbamate was 2.91 : 0.98 : 1.0 : 6.1, which shows that the molar ratio of cadaverine to carbon dioxide is almost 1 : 1.

FTIR spectra shown in Fig. 5a confirm the almost identical chemical composition of the crude and refined cadaverine carbamate. It shows that the refining process does not change the structure of the cadaverine carbamate. Thermo gravimetric analysis (TGA) of the refined cadaverine carbamate revealed one-stage decomposition (Fig. 5b). One-stage decomposition of the refined cadaverine carbamate exhibited that the dissociation temperature of carbon dioxide is consistent with that of the cadaverine gasification. During this stage, cadaverine carbamate loses 95% weight. The X-ray diffraction (XRD) result

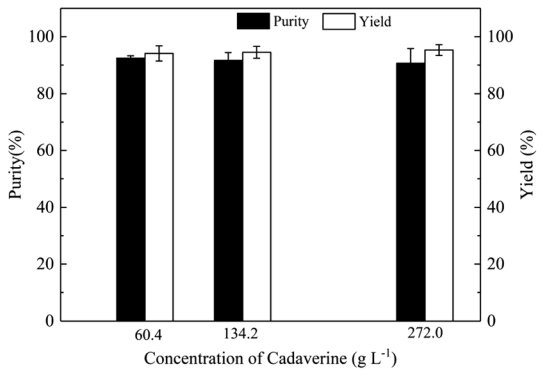

Fig. 3 Effects of the deprotonation cadaverine concentration in the *n*-butanol extraction solution on purity and yield of cadaverine carbamate.

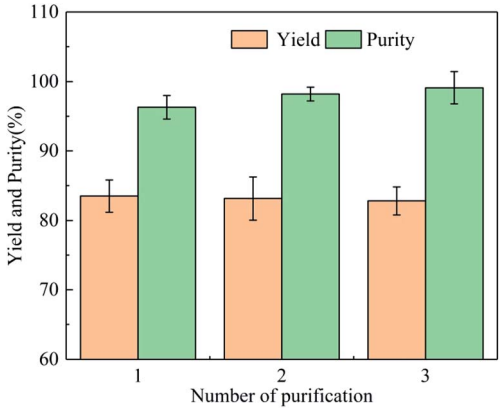

Fig. 4 Effect of the number of solventing-out crystallization on purity and yield of cadaverine carbamate.

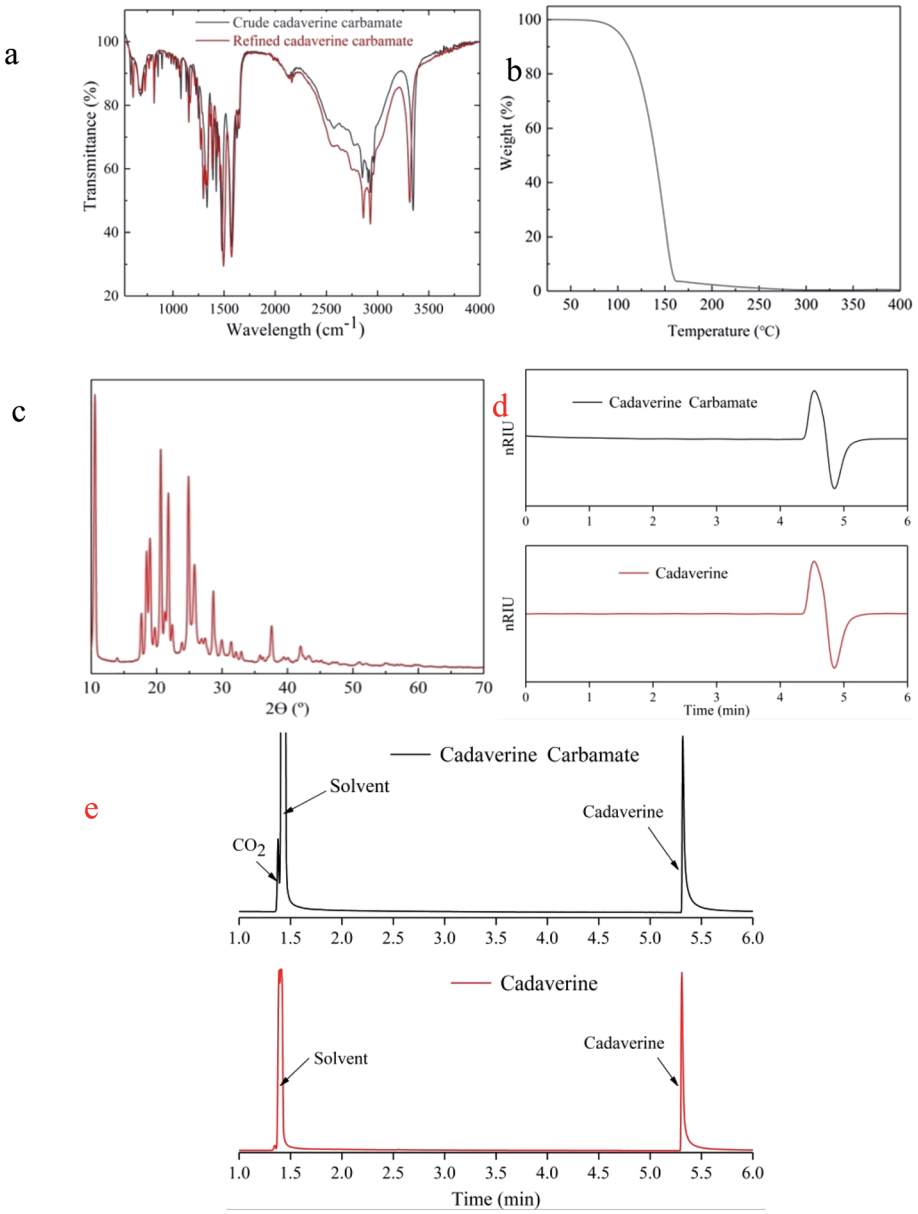

Fig. 5 (a) FTIR of crude and refined cadaverine carbamate; (b) TGA of refined cadaverine carbamate; (c) XRD of the refined cadaverine carbamate; (d) HPLC of the refined cadaverine carbamate and free cadaverine; (e) GC-MS spectroscopy of refined cadaverine carbamate and free cadaverine.

indicates that the refined cadaverine carbamate has obvious crystal peaks (Fig. 5c), indicating crystalline structure. In summary, purity of 99.1% of cadaverine carbamate was obtained by the amine absorption to capture carbon dioxide, and the high purity cadaverine carbamate obtained by solventing-out crystallization is crystalline in structure that can easily dissociate into carbon dioxide. HPLC profiles of the refined cadaverine carbamate and free cadaverine recorded using a differential refractometer detector (Fig. 5d) show that the refined cadaverine carbamate has high purity. GC-MS profiles of the refined cadaverine carbamate and free cadaverine in Fig. 5e and S1† indicate that the refined cadaverine carbamate was formed only by the combination of cadaverine and carbon dioxide.

^{13}C and ^{1}H NMR spectra of refined cadaverine carbamate and free cadaverine are shown in Fig. 6. Free cadaverine was dissolved in $CDCl_3$, while the refined cadaverine carbamate was insoluble in $CDCl_3$ but dissolved in D_2O. The carbonyl carbons in the refined cadaverine carbamate ($R\text{-}NH\text{-}COO^-$) were found with the signal of 164.81 ppm.[42,43] Cadaverine carbamate is formed by the reaction of free cadaverine with carbon dioxide. ^{13}C NMR allowed the identification of the forms for getting information of the mechanisms and reaction pathways between diamine and carbon dioxide.[44] It is found from Fig. 6 that the refined cadaverine carbamate can be found in three forms in D_2O: [$^-OOC\text{-}NH\text{-}(CH_2)_5\text{-}NH\text{-}COO^-$], [$^+NH_3\text{-}(CH_2)_5\text{-}NH_3^+$] and [$^+NH_3\text{-}(CH_2)_5\text{-}NH\text{-}COO^-$]. In comparison with free cadaverine,

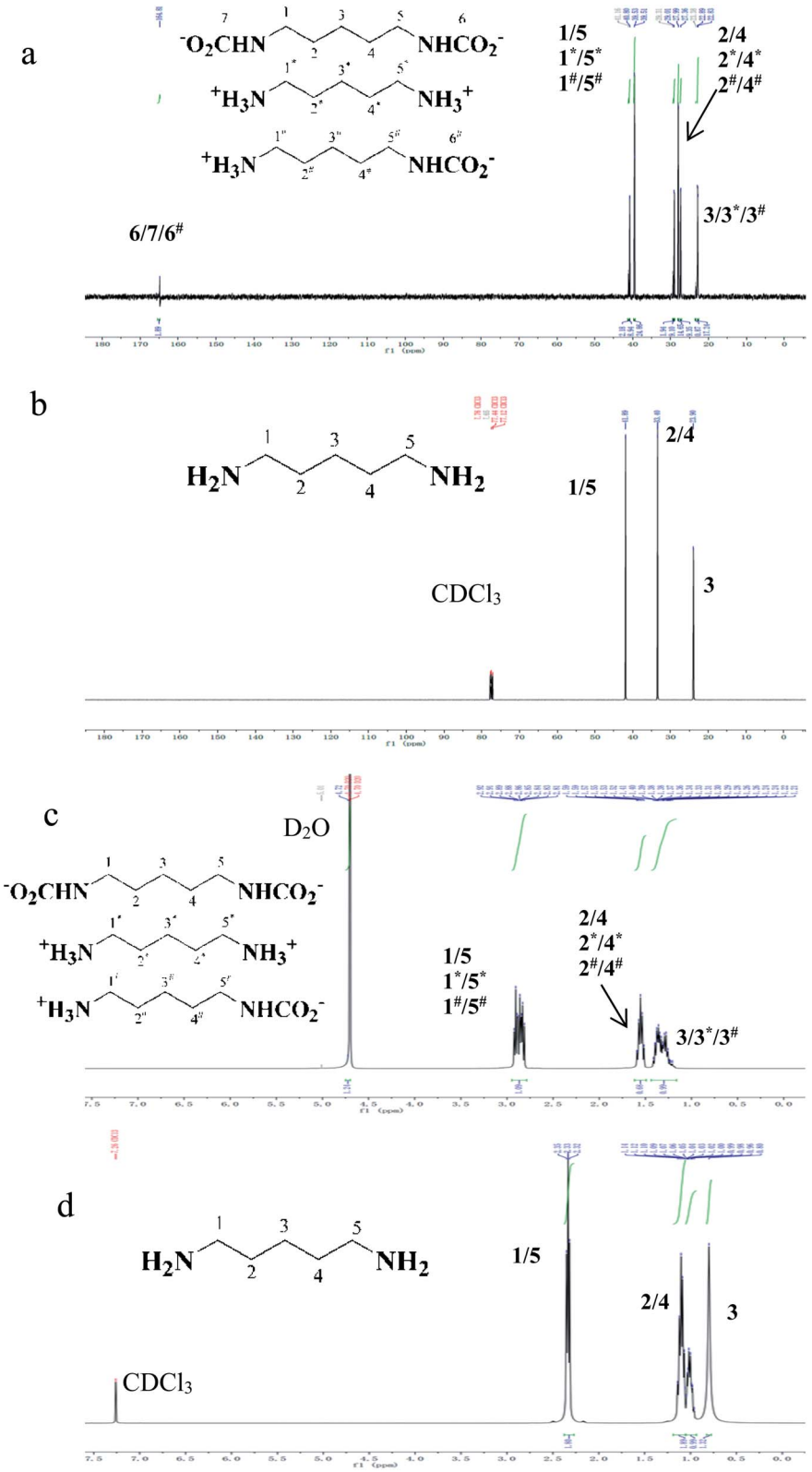

Fig. 6 ^{13}C NMR spectroscopy of refined cadaverine carbamate (a) and free cadaverine (b); ^{1}H NMR spectroscopy of refined cadaverine carbamate (c) and free cadaverine (d); refined cadaverine carbamate was dissolved in D_2O and free cadaverine was dissolved in $CDCl_3$.

the refined cadaverine carbamate has a variety of structural forms.

Conclusions

In this study, a green and sustainable separation of bio-based cadaverine based on the carbon dioxide capture *via* the formation of carbamate is developed. We used the bioconversion liquid of cadaverine as the raw material, the activated carbon discolored the concentrated cadaverine solution, and then the deprotonated cadaverine was extracted by *n*-butanol. The crude cadaverine carbamate was prepared by directly injecting carbon dioxide into the *n*-butanol extraction solution containing deprotonated cadaverine. Finally, refined cadaverine carbamate with a purity of 99.1% was obtained after three times of solventing-out crystallization with ethanol. Furthermore, the high purity cadaverine carbamate crystal technology provides a new idea for the separation of other bio-based amines.

CRediT authorship contribution statement

Hui Li: conceptualization, writing – original draft, writing – review & editing, funding acquisition, project administration, supervision. *Xu Xu*: investigation, methodology. *Weimin Tan*: project administration, supervision. *Xuedong Lu*: conceptualization, data curation. *Feng He*: investigation, methodology. *Sheng Xu*: conceptualization, supervision. *Weilong Tian*: visualization, methodology. *Kequan Chen*: funding acquisition, project administration. *Ganlu Li*: resources, project administration, supervision. *Pingkai Ouyang*: funding acquisition, project administration, resources, supervision. *Yaozong Liu*: resources, supervision. *Ruiyuan Liang*: resources, supervision.

Conflicts of interest

The authors declare no competing financial interest.

Acknowledgements

This work was supported by National Natural Science Foundation of China (21706126), National Key Research and Development Program (2016YFA0204300), Key Research and Development Program (Social Development) Project of Jiangsu Province (BE2018730).

Notes and references

1 W. Ma, K. Chen, Y. Li, N. Hao, X. Wang and P. Ouyang, *Engineering*, 2017, **3**, 308–317.
2 T. U. Chae, J. H. Ahn, Y. Ko, J. W. Kim, J. A. Lee, E. H. Lee and S. Y. Lee, *Metall. Eng.*, 2020, **58**, 2–16.
3 Y. K. Leong, C. Chen, S. Huang, H. Lin, S. Li, I. Ng and J. Chang, *Biochem. Eng. J.*, 2020, **157**, 107547.
4 R. Matsuura, M. Kishida, R. Konishi, Y. Hirata, N. Adachi, S. Segawa, K. Imao, T. Tanaka and A. Kondo, *Biotechnol. Bioeng.*, 2019, **116**, 2640–2651.
5 W. Olughu, A. Nienow, C. Hewittd and C. Rielly, *J. Chem. Technol. Biotechnol.*, 2020, **95**, 675–685.
6 J. Rui, S. You, Y. Zheng, C. Wang, Y. Gao, W. Zhang, W. Qi, R. Su and Z. He, *Bioresour. Technol.*, 2020, **302**, 122844.
7 C. Huang, W. Ting, Y. Chen, P. Wu, C. Dong, S. Huang, H. Lin, S. Li, I. Ng and J. Chang, *Biochem. Eng. J.*, 2020, **156**, 107514.
8 W. Ma, W. Cao, H. Zhang, K. Chen, Y. Li and P. Ouyang, *Biotechnol. Lett.*, 2015, **37**, 799–806.
9 V. F. Wendisch, M. Mindt and F. Pérez-García, *Appl. Microbiol. Biotechnol.*, 2018, **102**, 3583–3594.
10 G. Wei, A. Zhang, X. Lu, F. He, H. Li, S. Xu, G. Li, K. Chen and P. Ouyang, *J. CO_2 Util.*, 2020, **37**, 278–284.
11 M. Ammar, Y. Cao, P. He, L. Wang, J. Chen and H. Li, *Chin. J. Chem. Eng.*, 2017, **25**, 1760–1770.
12 H. T. Kim, K. Baritugo, S. M. Hyun, T. U. Khang, Y. J. Sohn, K. H. Kang, S. Y. Jo, B. K. Song, K. Park, I. Kim, Y. T. Hwang, S. Y. Lee, S. J. Park and J. C. Joo, *ACS Sustainable Chem. Eng.*, 2020, **8**, 129–138.
13 J. Feng, Q. Lu, W. Tan, K. Chen and P. Ouyang, *Front. Chem. Sci. Eng.*, 2019, **13**, 80–89.
14 F. Wang and C. E. Diesendruck, *Polym. Chem.*, 2017, **8**, 3712–3720.
15 M. Malik and R. Kaur, *Polym. Eng. Sci.*, 2018, **58**, 112–117.
16 Y. Cho and S. Hwang, *Polym. Bull.*, 2018, **75**, 5795–5807.
17 Y. Hong, H. Kim, J. Jeon, Y. Moon, J. Hong, J. Joo, B. Song, K. Park, S. Lee and Y. Yang, *J. Ind. Eng. Chem.*, 2018, **64**, 167–172.
18 S. Kind, S. Neubauer, J. Becker, M. Yamamoto, M. Volkert, G. Abendroth, O. Zelder and C. Wittmann, *Metall. Eng.*, 2014, **25**, 113–123.
19 A. Krzyżaniak, B. Schuur and A. B. de Haan, *J. Chem. Technol. Biotechnol.*, 2013, **88**, 1937–1945.
20 Y. Liu, Y. Zheng, H. Wu, W. Zhang, T. Ren, S. You, W. Qi, R. Su and Z. He, *J. Chem. Technol. Biotechnol.*, 2020, **9**, 1542–1549.
21 J. A. Lee, J. H. Ahn, I. Kim, S. Li and S. Y. Lee, *Chem. Eng. Sci.*, 2019, **196**, 324–332.
22 M. Gupta and H. F. Svendsen, *Int. J. Greenhouse Gas Control*, 2020, **98**, 103061.
23 X. Zhao, S. Yang, S. Ebrahimiasl, S. Arshadi and A. Hosseinian, *J. CO_2 Util.*, 2019, **33**, 37–45.
24 M. Zhang, M. Chen and Z. Ni, *Polymer*, 2020, **186**, 122009.
25 M. Gupta and H. F. Svendsen, *J. Phys. Chem. B*, 2019, **123**, 8433–8447.
26 A. F. M. Streit, L. N. Côrtes, S. P. Druzian, M. Godinho, G. C. Collazzo, D. Perondi and G. L. Dotto, *Sci. Total Environ.*, 2019, **660**, 277–287.
27 E. Zhou, Y. He, X. Ma, G. Liu, Y. Huang, C. Chen and W. Wang, *Chem. Eng. Process.*, 2017, **121**, 224–231.
28 D. Park, Y. Ju, J. Kim, H. Ahn and C. Lee, *Sep. Purif. Technol.*, 2019, **223**, 63–80.
29 R. Sanghi and P. Verma, *Color. Technol.*, 2013, **129**, 85–108.
30 S. Zaccaria, N. A. Boff, F. Bettin and A. J. P. Dillon, *Chem. Pap.*, 2019, **73**, 3085–3094.
31 A. P. Rawat, V. Kumar and D. P. Singh, *Sep. Sci. Technol.*, 2020, **55**, 907–921.

32 M. Kavand, M. Soleimani, T. Kaghazchi and N. Asasian, *Chem. Eng. Commun.*, 2016, **203**, 123–135.
33 R. Cao, J. Guo, X. Hua and Y. Xu, *Food Chem.*, 2020, **310**, 125934.
34 H. Li and Z. Wang, *RSC Adv.*, 2015, **5**, 30711–30718.
35 S. Li, K. Song, D. Zhao, J. R. Rugarabamu, R. Diao and Y. Gu, *Microporous Mesoporous Mater.*, 2020, **302**, 110220.
36 Y. Matsuzaki, H. Yamada, F. A. Chowdhury, S. Yamamoto and K. Goto, *Ind. Eng. Chem. Res.*, 2019, **58**, 3549–3554.
37 V. H. Shah, V. Pham, P. Larsen, S. Biswas and T. Frank, *Ind. Eng. Chem. Res.*, 2016, **55**, 1731–1739.
38 A. Bednarz, A. Jupke, A. C. Spieß and A. Pfennig, *J. Chem. Technol. Biotechnol.*, 2019, **94**, 426–434.
39 A. Bednarz, A. C. Spieß and A. Pfennig, *J. Chem. Technol. Biotechnol.*, 2017, **92**, 1817–1824.
40 X. Tian, M. X. Huo, D. J. Bian, Y. Zuo and S. S. Ai, *Desalin. Water Treat.*, 2016, **57**, 382–387.
41 K. Chen, B. Cao, J. Zhu, B. Wu and L. Ji, *Asia-Pac. J. Chem. Eng.*, 2009, **4**, 832–836.
42 E. Skylogianni, C. Perinu, B. Y. C. Gameros and H. K. Knuutil, *J. Chem. Thermodyn.*, 2020, **151**, 106176.
43 F. Barzagli, C. Giorgi, F. Mani and M. Peruzzini, *ACS Sustainable Chem. Eng.*, 2020, **8**, 14013–14021.
44 X. E. Hu, Q. Yu, F. Barzagli, C. Li, M. Fan, K. A. M. Gasem, X. Zhang, E. Shiko, M. Tian, X. Luo, Z. Zeng, Y. Liu and R. Zhang, *ACS Sustainable Chem. Eng.*, 2020, **8**, 6173–6193.